Available online at www.sciencedirect.com
ScienceDirect
Journal of the European Ceramic Society 31 (2011) 2351–2356
www.elsevier.com/locate/jeurceramsoc

Chemical expansion of nonstoichiometric $Pr_{0.1}Ce_{0.9}O_{2-\delta}$: Correlation with defect equilibrium model

Sean R. Bishop [a,*], Harry L. Tuller [a], Yener Kuru [a,b], Bilge Yildiz [b]

[a] Department of Materials Science and Engineering, Massachusetts Institute of Technology, 77 Massachusetts Ave #13-3126, Cambridge, MA 02139, USA
[b] Department of Nuclear Science and Engineering, Massachusetts Institute of Technology, 77 Massachusetts Ave #24-210, Cambridge, MA 02139, USA

Received 24 March 2011; accepted 22 May 2011

Abstract

Undoped and acceptor doped cerium dioxide is known to exhibit non-stoichiometry induced chemical expansion at elevated temperatures and reducing environments with impact on the mechanical integrity of solid oxide fuel cells and permeation membranes. In this paper, the chemical expansion of $Pr_{0.1}Ce_{0.9}O_{2-\delta}$ is measured and analyzed with respect to its defect equilibria and the chemical coefficient of expansion, analogous to thermal coefficient of expansion, is extracted. The addition of Pr to CeO_2 leads to major deviations from stoichiometry, and correspondingly to large chemical expansions, under readily accessible experimental conditions (e.g. in air at elevated temperatures). $Pr_{0.1}Ce_{0.9}O_{2-\delta}$, therefore, serves as a model system for studying chemical expansion in ceria-based solid solutions in order to predict the conditions in which they exhibit suppressed chemical expansion.

Keywords: CeO_2; Chemical properties; Mechanical properties; Thermal properties; Chemomechanics

1. Introduction

Cerium dioxide crystallizes in the fluorite structure, and like stabilized zirconia, can accommodate a high oxygen deficiency by the substitution of lower valent elements on the cation sublattice, e.g. Gd'_{Ce}. This leads to the high oxygen ion conductivities in Gd doped ceria (GDC) and its interest as a solid electrolyte in solid oxide fuel cells (SOFCs).[1] At the same time, ceria, CeO_2, is also well known to release significant levels of oxygen at low oxygen partial pressures (P_{O_2}) and elevated temperatures (e.g. $<\sim 10^{-15}$ atm O_2 at 800 °C) leading to mixed ionic electronic conductivity (MIEC). This can be described by the following defect reaction, written in Kröger–Vink notation.[2]

$$O_O^{\times} \leftrightarrow V_O^{\bullet\bullet} + 2e' + \frac{1}{2}O_2(g) \quad (1)$$

where $O_O^{\times}$, $V_O^{\bullet\bullet}$, and e' are oxide ions in the lattice, doubly charged oxygen vacancies, and electrons in the conduction band made up of Ce 4f energy states, respectively.[3] The electrons formed during reduction are often treated as being localized on cerium, thereby converting Ce^{4+} to Ce^{3+} ions. This is consistent with the demonstration that electrons in ceria can be described as small polarons, i.e. they move through the lattice via a thermally activated hopping process.[4] Perhaps less appreciated is that, associated with the loss of oxygen, a significant dilation in the crystalline lattice occurs upon reduction.[5–7] This can lead to a major build-up of stresses in SOFC and oxygen permeation membrane structures and, if not properly compensated for, lead ultimately to device failure.[8–10] In this study, the correlation between thermally and chemically induced changes in lattice parameter and the oxygen nonstoichiometry (δ) in the solid solution $Pr_{0.1}Ce_{0.9}O_{2-\delta}$ (PCO) is investigated. PCO serves as a model system for such studies since there are experimental regimes, on the one hand, at reduced P_{O_2} for which Pr acts in a similar fashion to Gd, as a fixed valent dopant, with little change in the oxygen vacancy concentration with changes in temperature and P_{O_2}, and on the other hand, under oxidizing conditions for which the oxygen vacancy concentration becomes strongly dependent on temperature and P_{O_2}. This leads to an observed 2–3 times increase in the thermal expansion coefficient due to oxygen loss upon heating.[11–13] Additionally, at high P_{O_2} and sufficiently high Pr concentration (including the

* Corresponding author. Tel.: +1 617 253 5002; fax: +1 781 258 5749.
E-mail address: srbishop@mit.edu (S.R. Bishop).

0955-2219/$ – see front matter © 2011 Elsevier Ltd. All rights reserved.
doi:10.1016/j.jeurceramsoc.2011.05.034

level studied here), PCO exhibits mixed ionic electronic conductivity (MIEC), a characteristic of high performance SOFC cathode materials.[14–16] This has led to the study of PCO as an SOFC cathode and oxygen permeation membrane, thus requiring characterization of its chemical expansion among other thermochemical properties.[17,18]

Upon the substitution of Ce by Pr in PCO, the loss of oxygen (i.e. increased δ) from the lattice upon heating and/or exposure to reducing conditions, initiates at much higher P_{O_2} than in undoped ceria. This reaction, resulting from the reduction of Pr, may be described by:

$$O_O^{\times} + 2Pr_{Ce}^{x} \leftrightarrow V_O^{\bullet\bullet} + 2Pr_{Ce}^{\prime} + \frac{1}{2}O_2(g) \quad (2)$$

where Pr_{Ce}^{x} and $Pr_{Ce}^{\prime}$ are Pr^{4+} and Pr^{3+} ions substituting on Ce ion sites, respectively. When Eq. (2) dominates defect generation (for $P_{O_2} > 10^{-18}$ atm O_2 at 700 °C), charge neutrality requires that:

$$[Pr_{Ce}^{\prime}] \approx 2[V_O^{\bullet\bullet}] \quad (3)$$

As mentioned earlier, undoped and ceria doped with fixed valent acceptor dopants (e.g. Gd^{3+}) are reported to exhibit lattice dilation with increasing δ, termed *chemical expansion*. The chemical expansion is believed to originate from the increase in radius of cations upon reduction and/or electrostatic considerations upon removal of oxygen, both mechanisms occurring simultaneously (Eq. (3) for PCO), and is not specific to ceria or fluorites, occurring also, for example, in transition metal systems for high temperature SOFCs to low temperature superconductor materials.[19,20]

Analogous to the thermal coefficient of expansion, a chemical coefficient of expansion (α_C) can be defined through the following equation.

$$\varepsilon_C = \alpha_C(\delta - \delta_{ref}) \quad (4)$$

where ε_C is the chemical expansion induced by non-stoichiometry δ relative to a reference δ_{ref}. Written in terms of δ, α_C is unitless. It has been observed in undoped and Gd doped ceria, that α_C is a decreasing function of δ (but insensitive to temperature) and this is believed to be the result of defect interactions leading to clusters or complexes of defects at high δ.[5,6] In recent thermodynamic and electrical modeling of PCO, such defect complexes were found to be unnecessary or inconsistent with defect equilibria and conductivity measurements.[14,21,22] Therefore, in the present investigation of chemical expansion, it is expected that α_C will be a constant with respect to the Pr reduction reaction (Eq. (2)).

Previous researchers have measured the thermo-chemical expansion of PCO, typically heating and cooling the sample in air and observing the linear length change by dilatometry or high temperature X-ray diffraction (HTXRD).[13,23–25] While these measurements show the large effect of chemical expansion when qualitatively compared to oxygen loss, α_C was not derived. To the authors' knowledge, in only one instance was α_C for PCO determined, using stoichiometry measured by coulometric titration and thermogravimetry with length change measured by dilatometry at 800 °C for $Pr_{0.2}Ce_{0.8}O_{2-\delta}$.[12] In this paper, we use our previously developed defect equilibria model,[14] experimentally verified through thermo-gravimetry and electrical conductivity measurements, along with dilatometry and HTXRD to determine α_C in $Pr_{0.1}Ce_{0.9}O_{2-\delta}$ over 1 atm $< P_{O_2} < \sim 10^{-16}$ atm from 650 to 900 °C and then use these results to model the thermo-chemical expansion.

2. Material and methods

Sample preparation is detailed in a previous report[14] with a brief description given here. Pr and Ce nitrates were precipitated using oxalic acid with the precipitate calcined at elevated temperature (>700 °C) to form single phase $Pr_{0.1}Ce_{0.9}O_{2-\delta}$ as confirmed by X-ray diffraction and wavelength dispersive spectroscopy. The powder was pressed into a disk that was sintered at >1400 °C to yield a >95% dense specimen that was subsequently cut into a 10.9 mm long rectangular bar with an approximately 2 mm × 2 mm cross section. Samples previously used for both thermogravimetric analysis and conductivity measurements were prepared from the same pellet.[14]

Dilatometry was performed on the rectangular specimen using a single pushrod dilatometer (Automatic recording dilatometer; Edward Orton, Jr. Ceramic Foundation). An undoped ceria sample was prepared in a similar fashion and used as a reference in the dilatometer. The error in expansion is estimated to be ±0.008%. The P_{O_2} was controlled by use of appropriate mixtures of O_2/N_2 and CO/CO_2 and the P_{O_2} of the gases was confirmed with an in situ yttria stabilized zirconia Nernst type electromotive force sensor.

3. Results

The sample expansion (ε) was calculated using the formula

$$\varepsilon = \frac{\Delta l}{l_o} = \frac{p - p_{ref}}{l_o} \quad (5)$$

where p is the sample position (read from the dilatometer output) at the set temperature and P_{O_2}, p_{ref} is a reference, or starting, position, and l_o is the sample length at room temperature after annealing in air. For the magnitude of expansion measured here, defining p_{ref} at a length other than l_o results in a maximum error of ~1% of expansion and is similar to the inaccuracy in measuring l_o. There was no measurable dependence of the dilatometer measurements on gas composition. At 900 °C, the dilatometer displayed an anomalous long term expansion, presumably from the quartz sample holder and pushrod which was accounted for as discussed in a previous work and not observed at any of the lower temperatures.[19]

The variations in ε of the $Pr_{0.1}Ce_{0.9}O_{2-\delta}$ (PCO) specimen for various programmed changes in temperature and atmosphere are shown in Fig. 1 (see figure caption). Also shown is the temperature induced expansion of undoped ceria, derived from neutron diffraction studies by Yashima et al.,[26] along with their second order polynomial fit to the data

$$\varepsilon_T = 2.64 \times 10^{-7}\Delta T^2 + 9.41 \times 10^{-4}\Delta T + 5.32 \times 10^{-2} \quad (6)$$

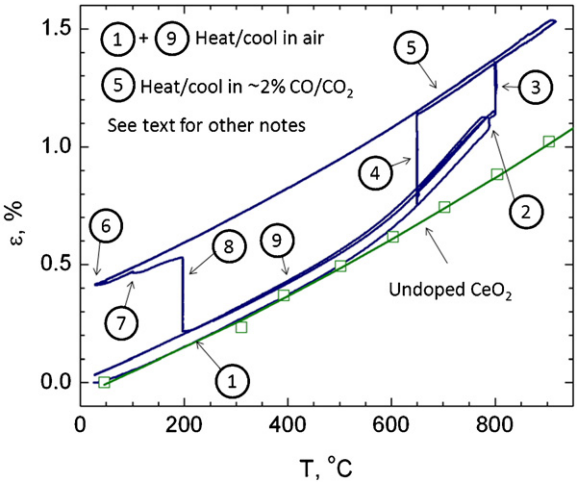

Fig. 1. Measured expansion of $Pr_{0.1}Ce_{0.9}O_{2-\delta}$ as a function of temperature and atmosphere. Numbered regions are described in the article text. Square points represent expansion of undoped ceria from reference[26] shown with a second order polynomial fit given by Eq. (6).

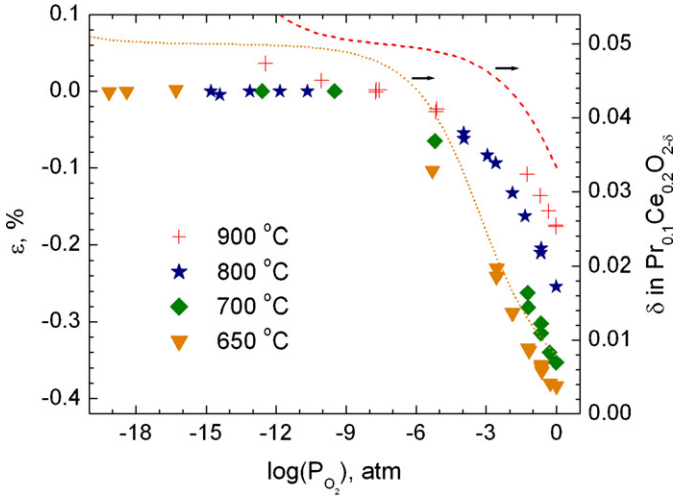

Fig. 3. Isothermal expansion (points) measured here and δ from cited defect equilibria model (dotted – 650 °C; dashed – 900 °C) for $Pr_{0.1}Ce_{0.9}O_{2-\delta}$ plotted against P_{O_2}.[14] Below 900 °C, expansion exhibits a plateau at low P_{O_2} where $\delta \approx 0.05$, the defined sample reference position (p_{ref}). Error in expansion is similar to size of data points.

The purpose of Fig. 1 is to introduce the thermo-chemical expansion measurement to the reader with indication of important features discussed throughout this article. At ~550 °C, there is a clear positive deviation of ε for PCO from undoped ceria upon heating in air ((1), in the figure) and, as explained below, this deviation is due to the reduction of Pr and the formation of oxygen vacancies (Eq. (2)). At (3) and (4) in Fig. 1, the P_{O_2} was varied isothermally in order to isolate chemical expansion from thermal expansion. Fig. 2 shows the isothermal chemical expansion measured at 650 °C corresponding to (4) in Fig. 1. During this part of the measurement, the sample reversibly expands following a decrease in P_{O_2} and contracts following an increase in P_{O_2}. The equilibrium expansion at each P_{O_2}, along with δ, predicted using our previously developed defect equilibria model, is plotted in Fig. 3. At each temperature (except for 900 °C), ε reaches a plateau value as P_{O_2} drops below $\sim 10^{-9}$ atm. The same phenomenon has been observed for both the electrical conductivity and oxygen non-stoichiometry in PCO, and is attributed to the condition at which all of the Pr has been reduced to the trivalent state, leading to a fixed oxygen deficiency corresponding to $\delta \approx 0.05$ in $Pr_{0.1}Ce_{0.9}O_{2-\delta}$.[14] This plateau was thus chosen to serve as p_{ref} for each temperature and so the percent contraction of each sample with increase in P_{O_2} is then referenced to the same δ. In order to determine p_{ref} at 900 °C, our previously developed defect chemistry model was used to calculate the P_{O_2} at which $\delta \approx 0.05$.[14] For this temperature, the sample shows expansion beyond the plateau at low P_{O_2} due to the onset of Ce reduction to the trivalent state (Eq. (1)).

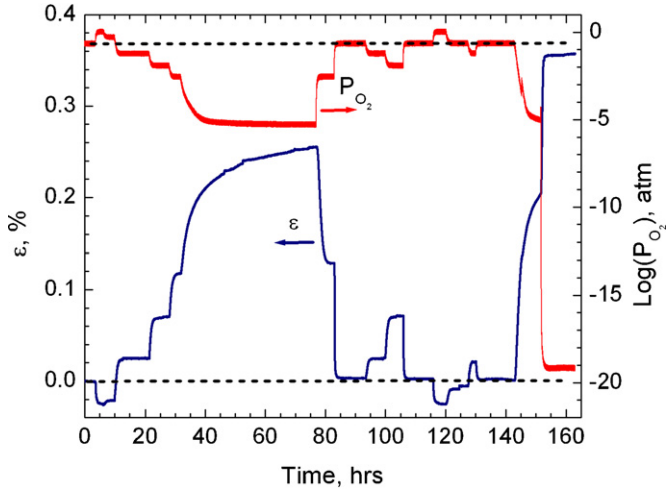

Fig. 2. Isothermal chemical expansion of $Pr_{0.1}Ce_{0.9}O_{2-\delta}$ at 650 °C ((4) in Fig. 1) corresponding to the step changes in P_{O_2}. The dashed lines indicate the P_{O_2} and sample dimension for air, showing reversibility of sample.

After performing the isothermal expansion, (4) in Fig. 1, the sample was heated and then cooled to room temperature, (5), in ~2% CO/CO_2 which corresponds to approximately the lowest P_{O_2} for which the plateau region ($\delta \approx 0.05$) is reached in Fig. 3. Under these conditions, nearly no changes in stoichiometry should occur and so, mostly thermal expansion is observed. Indeed this is consistent with the fact that expansion during (5) is much less than in (1) at temperatures above 550 °C. At (6), the highly reduced state, $\delta \approx 0.05$ is frozen in so that it shows a longer dimension (~0.4%) than the initial condition (i.e. sample cooled in air). Following this point, the atmosphere was changed from CO/CO_2 to air and the specimen was heated to 100 °C, (7), and held isothermally for 15 h, resulting only in a slight contraction due to partial reoxidation. The sample was then heated to 200 °C and held isothermally, (8), for 70 h during which time the sample contracted considerably from oxidation. Finally, heating was resumed, (9), to 800 °C in air, after which the sample was cooled to room temperature. The heating/cooling of (9) shows reversible behavior and is only offset from the original heating cycle, (1), by an initial length change that occurred at (2), presumably due to shifting of the sample in the dilatometer. This analysis highlights the ability to induce expansion in PCO both thermally and chemically while maintaining reversible behavior. In the following discussion, the chemical expansion coefficient,

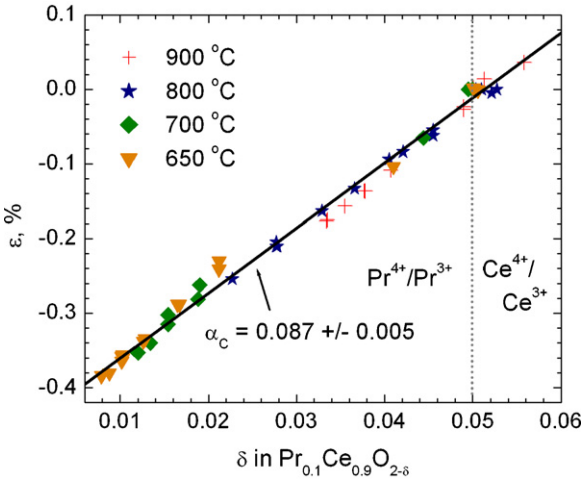

Fig. 4. Isothermal expansion of PCO (Fig. 2) plotted against δ determined using the defect chemistry model. Data sets show little dependence on temperature and the solid line is a linear fit to all the data with chemical expansion coefficient, α_C, shown. Error in expansion is similar to the size of data points.

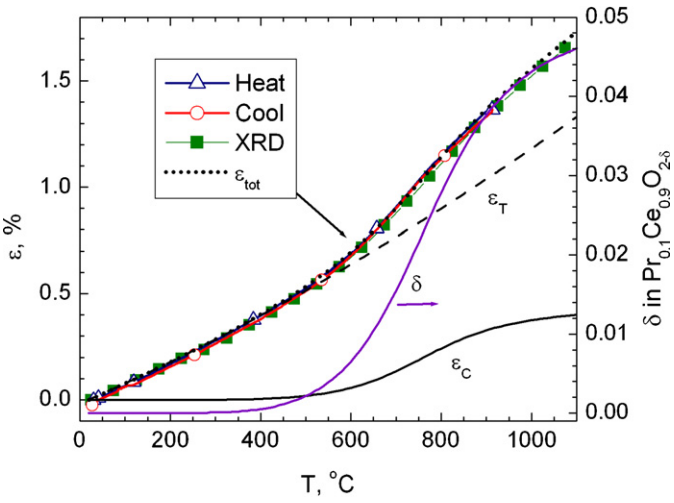

Fig. 5. Expansion versus temperature in air, showing modeled thermal (ε_T), chemical (ε_C), and total (ε_{tot}) expansion. Open triangles and squares are from the present dilatometric work (ε error is similar to the size of data points), closed squares are from HTXRD.[30] Calculated non-stoichiometry (δ) is plotted on the right axis.

α_C, is derived and used to predict the thermo-chemical expansion of PCO.

4. Discussion

Fig. 4 shows the isothermal expansion of Fig. 3 replotted against δ (with the δ - P_{O_2} relationship obtained from the defect equilibria model). In the figure, each expansion data set is observed to follow an approximate linear relationship with δ. Eq. (4) was fit to all the expansion data, yielding $\varepsilon_C = 0.087 \pm 0.005$ (uncertainty based on error in reported expansion), using $\delta_{ref} = 0.05$. The point at which the reduction reaction switches from Eq. (1)–(2) (δ_{ref}) is also indicated in the figure. As mentioned in the introduction, α_C was found to have a non-linear dependence on δ for highly reducing conditions in undoped and Gd doped ceria believed to be the result of defect interactions. Significant non-linearity is not observed here, consistent with the assumption of non-interacting defects, or at least, no apparent change in the level of defect interaction. In addition, there is little to no temperature dependence of α_C, also observed in other systems.[5,19]

The value of α_C measured here (0.087) is less than that reported for undoped and Gd doped ceria (0.1–0.18), but agrees well with values for $Pr_{0.2}Ce_{0.8}O_{2-\delta}$ (0.084).[6,12,27,28] Lattice dilation, upon reduction, must derive from a superposition of lattice dimensional changes induced by the formation of oxygen vacancies (resulting in electrostatic repulsion of surrounding cations and in electrostatic contraction of surrounding anions) and the reduction of Pr^{4+} to Pr^{3+} (resulting in an ionic radius increase). The changes in crystal radii of Pr and Ce upon reduction of quadrivalent to trivalent valence in 8-fold coordination are 15.1% (Pr) and 15.6% (Ce), respectively.[29] Therefore, the trend of smaller α_C of Pr versus Ce upon reduction agrees with the difference in crystal radius change.

Since the chemical expansion coefficient is now defined, it becomes possible to predict the thermo-chemical expansion (ε_{tot}) of PCO in air, as shown in Fig. 5 along with measurements performed by dilatometry here and HTXRD from the literature.[30] ε_{tot} in air was predicted by summing the thermal (ε_T from Eq. (6)) and chemical (ε_C) contributions of expansion as a function of temperature at constant P_{O_2} by the following equation.

$$\varepsilon_{tot} = \varepsilon_T + \varepsilon_{C,P_{O_2}} = \alpha_T \Delta T + \alpha_C \Delta \delta_{P_{O_2}} \quad (7)$$

where the subscript P_{O_2} denotes constant oxygen partial pressure (air) and so the change in δ is only due to temperature. The modeled and measured data show nearly identical behavior and the anomalous high temperature deviation from thermal expansion is explained by the added contribution from the chemical expansion component. It is worth mentioning that the agreement between expansion measured by dilatometry matches that from HTXRD, showing that the chemical expansion is related primarily to the change in lattice parameter and not significantly influenced by interfacial volume changes or a different defect mechanism than proposed here (e.g. Schottky).[31,32]

The derivative of the total expansion with respect to temperature (the thermo-chemical expansion coefficient, α) for heating and cooling of PCO in air, cooling in 2% CO/CO_2 (curve (5) in Fig. 1), and the HTXRD data in air from reference[30] are shown in Fig. 6. All samples show similar α below 500 °C in agreement with pure thermal expansion. Above 500 °C in air, PCO shows a large positive deviation from undoped ceria as a result of the chemical expansion, amounting to more than a 2 fold increase in α, at the peak. Such a large increase in α highlights the importance of quantifying the chemical expansion for device design, especially in composite systems typical of SOFCs.

α associated with heating PCO in air (α_{tot}) is modeled in the figure using the summation of the thermal expansion (α_T) and the effective chemical expansion coefficients (α_C^*). α_T and α_C^* were derived by differentiating their respective contributions to Eq. (7). The chemical expansion contribution shows a peak at the

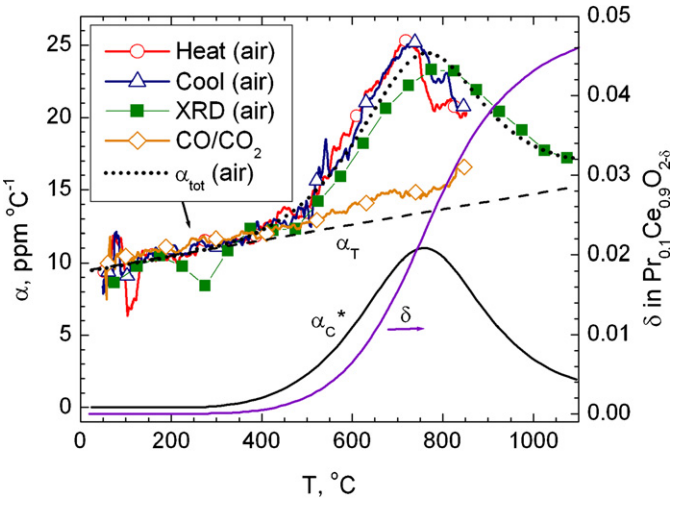

Fig. 6. Expansion coefficients for $Pr_{0.1}Ce_{0.9}O_{2-\delta}$ as a function of temperature with non-stoichiometry (δ) plotted on the right axis. Atmosphere conditions for measurements and predicted total expansion coefficient (α_{tot}) are indicated in parentheses. Predicted values for α_T, α_C^*, and δ are for air atmosphere.

same temperature as the inflection in δ, where the rate of oxygen loss with increasing temperature begins to decrease, ultimately tailing off to zero when $\delta \approx 0.05$ (not measured or shown). As in Fig. 5, there is generally good agreement between the data obtained by HTXRD and dilatometry in Fig. 6. Differences may arise from small errors in temperature measurements for both the dilatometry and XRD measurement leading to noise in the numerical differentiation of expansion to obtain α as well as reduced number of data points in the lattice parameter measurement. It is gratifying to see that isothermally obtained α_C (Fig. 4) when combined with thermal expansion data on undoped ceria and our group's previously defined defect equilibria model for PCO, leads to such consistency in the modeling of ε_{tot} and α_{tot}.

It has been reported that the thermal expansion coefficient of PCO appears to increase with increasing δ, though not modeled in this work.[12,30] It should be mentioned that while the expansion measured by HTXRD of powder matched that of dense, bulk sample dilatometry quite well, there are subtle differences evident in Fig. 6. For example, in Fig. 6 if α_C (and hence α_C^*) is decreased slightly, α_{tot} would have a better fit to the initial increase in chemical expansion of the HTXRD curve, but then an increased α_T would be needed to fit the rest of the curve at higher temperature (>750 °C). It is possible that there is a slight difference between bulk expansion and powder expansion, presumably due to generation of defects at surfaces/interfaces and remains to be studied in future work.

In order to decrease the effects of chemical expansion, PCO could be operated strictly in a reducing atmosphere, while at $T < 200$ °C that atmosphere could be changed without significantly affecting stoichiometry due to "frozen-in" defects. As mentioned earlier, curve (5) in Fig. 1 and line "CO/CO_2" in Fig. 6 show the expansion and expansion coefficient measured for PCO during cooling in 2% CO/CO_2. The effect of chemical expansion is markedly reduced since the sample remains in a state where δ remains near 0.05. Taking the difference between initial sample position at the start of the experiment (prior to (1)) and sample position at point (6) in Fig. 1 and using α_C with Eq. (4), one finds that $\Delta\delta = 0.044$, showing a significant amount of "frozen-in" defects at room temperature. Upon heating the sample in air, not until 200 °C (point (8)) does a large amount of reoxidation occur with the kinetics of this oxidation step discussed in reference.[33] Therefore, by taking advantage of known thermodynamic equilibria, the operating conditions in which PCO exhibits either very large or quite small chemical expansion can be predicted.

5. Conclusions

The non-stoichiometry dependent chemical expansion was described in terms of the defect equilibria in $Pr_{0.1}Ce_{0.9}O_{2-\delta}$. Using isothermal measurements (650–900 °C) in a range of oxygen partial pressures (10^{-16}–1 atm), the chemical coefficient of expansion, α_C, was derived. α_C for Pr reduction agrees well with values derived for cerium reduction, though slightly less in accordance with their crystal radii change upon reduction. In addition, α_C was not found to have a significant dependence on δ, indicating limited contributions from defect interactions, consistent with previous defect equilibria modeling assumptions. The thermo-chemical expansion in air was modeled by utilizing the derived value for α_C along with thermal expansion data for undoped ceria. By having developed such an understanding of this system, the level of expansion can be predicted and controlled for given experimental conditions.

Acknowledgements

This research was funded by Basic Energy Sciences, Department of Energy under award DE-SC0002633 and the MIT Energy Initiative Seed Program.

References

1. Steele BCH. Appraisal of $Ce_{1-y}Gd_yO_{2-y/2}$ electrolytes for IT-SOFC operation at 500 degrees C. *Solid State Ionics* 2000;**129**:95–110.
2. Kroger FA, Vink HJ. Relations between the concentrations of imperfections in crystalline solids. *Solid State Phys* 1956;**3**:307–435.
3. Tuller HL, Nowick AS. Defect structure and electrical-properties of non-stoichiometric CeO_2 single-crystals. *J Electrochem Soc* 1979;**126**:209–17.
4. Tuller HL, Nowick AS. Small polaron electron-transport in reduced CeO_2 single-crystals. *J Phys Chem Solids* 1977;**38**:859–67.
5. Bishop SR, Duncan KL, Wachsman ED. Surface and bulk oxygen non-stoichiometry and bulk chemical expansion in gadolinium-doped cerium oxide. *Acta Mater* 2009;**57**:3596–605.
6. Bishop SR, Duncan KL, Wachsman ED. Defect equilibria and chemical expansion in non-stoichiometric undoped and gadolinium-doped cerium oxide. *Electrochim Acta* 2009;**54**:1436–43.
7. Adler SB. Chemical expansivity of electrochemical ceramics. *J Am Ceram Soc* 2001;**84**:2117–9.
8. Sato K, Omura H, Hashida T, Yashiro K, Yugami H, Kawada T, et al. Tracking the onset of damage mechanism in ceria-based solid oxide fuel cells under simulated operating conditions. *J Test Eval* 2006;**34**:246–50.
9. Krishnamurthy R, Sheldon BW. Stresses due to oxygen potential gradients in non-stoichiometric oxides. *Acta Mater* 2004;**52**:1807–22.
10. Atkinson A. Chemically-induced stresses in gadolinium-doped ceria solid oxide fuel cell electrolytes. *Solid State Ionics* 1997;**95**:249–58.
11. Bishop SR, Chen D, Kuru Y, Kim J-J, Stefanik TS, Tuller HL. Measurement and modeling of electrical, mechanical, and chemical properties of

a model mixed ionic electronic conductor: Pr doped Ceria. *ECS Trans* 2011;**33**:51–7.
12. Chatzichristodoulou C, Hendriksen PV, Hagen A. Defect chemistry and thermomechanical properties of $Ce_{0.8}Pr_xTb_{0.2-x}O_{2-\delta}$. *J Electrochem Soc* 2010;**157**:B299–307.
13. Fagg DP, Marozau IP, Shaula AL, Kharton VV, Frade JR. Oxygen permeability, thermal expansion and mixed conductivity of $Gd_xCe_{0.8-x}Pr_{0.2}O_{2-\delta}$, $x = 0$, 0.15, 0.2. *J Solid State Chem* 2006;**179**:3347–56.
14. Bishop SR, Stefanik TS, Tuller HL. Electrical conductivity and defect equilibria of $Pr_{0.1}Ce_{0.9}O_{2-\delta}$. *Phys Chem Chem Phys* 2011;**13**: 10165–73.
15. De Souza RA, Kilner JA. Oxygen transport in $La_{1-x}Sr_xMn_{1-y}Co_yO_{3\pm\delta}$ perovskites. Part II. Oxygen surface exchange. *Solid State Ionics* 1999;**126**:153–61.
16. Adler SB. Factors governing oxygen reduction in solid oxide fuel cell cathodes. *Chem Rev* 2004;**104**:4791–843.
17. Chen D., Bishop SR.and Tuller H.L. Oxygen surface exchange resistance of Pr-CeO_2 thin films. in preparation.
18. Chiba R, Komatsu T, Orui H, Taguchi H, Nozawa K, Arai H. SOFC cathodes composed of $LaNi_{0.6}Fe_{0.4}O_3$ and Pr-doped CeO_2. *Electrochem Solid State Lett* 2009;**12**:B69–72.
19. Bishop SR, Duncan KL, Wachsman ED. Thermo-chemical expansion in strontium-doped lanthanum cobalt iron oxide. *J Am Ceram Soc* 2010;**93**:4115–21.
20. Kuru Y, Usman M, Cristiani G, Habermeier H. Microstructural changes in epitaxial $YBa_2Cu_3O_{7-\delta}$ thin films due to creation of O vacancies. *J Cryst Growth* 2010;**312**:2904–8.
21. Chatzichristodoulou C, Hendriksen PV. Oxygen nonstoichiometry and defect chemistry modeling of $Ce_{0.8}Pr_{0.2}O_{2-\delta}$. *J Electrochem Soc* 2010;**157**:B481–9.
22. Stefanik T.S. Electrical Properties and Defect Structure of Praseodymium-Cerium Oxide Solid Solutions, Ph. D., Massachusetts Institute of Technology, Cambridge, MA, 2004.
23. Fagg DP, Kharton VV, Shaula A, Marozau IP, Frade JR. Mixed conductivity, thermal expansion, and oxygen permeability of $Ce(PrZr)O_{2-\delta}$. *Solid State Ionics* 2005;**176**:1723–30.
24. Ostroushko AA, Russkikh OV, Petrova SA, Zakharov RG, Prosvetova MV. Phase composition and thermal properties of Ce_{1-x} $Ln_{(x)}$ O_{2-d} (Ln = Sm, Pr) solid solutions. *Inorg Mater* 2010;**46**:959–64.
25. Nauer M, Ftikos C, Steele BCH. An evaluation of Ce-Pr Oxides and Ce-Pr-Nb oxides mixed conductors for cathodes of solid oxide fuel-cells - Structure, thermal-expansion and electrical-conductivity. *J European Ceram Soc* 1994;**14**:493–9.
26. Yashima M, Kobayashi S, Yasui T. Crystal structure and the structural disorder of ceria from 40 to 1497 degrees C. *Solid State Ionics* 2006;**177**:211–5.
27. Bishop SR, Duncan KL, Wachsman ED. Surface and bulk defect equilibria in strontium-doped lanthanum cobalt iron oxide. *J Electrochem Soc* 2009;**156**:B1242–8.
28. Mogensen M, Sammes NM, Tompsett GA. Physical, chemical and electrochemical properties of pure and doped ceria. *Solid State Ionics* 2000;**129**:63–94.
29. Shannon RD. Revised effective ionic-radii and systematic studies of interatomic distances in halides and chalcogenides. *Acta Crystallogr Sect A* 1976;**32**:751–67.
30. Kuru Y., Bishop S.R., Kim J.-J., Yildiz B. and Tuller H.L. Chemomechanical properties and microstructural stability of nanocrystalline Pr-doped ceria: an *in situ* X-ray diffraction investigation. Solid State Ionics, in press. doi:10.1016/j.ssi.2011.04.012.
31. Chiang HW, Blumenthal RN, Fournelle RA. A high-temperature lattice-parameter and dilatometer study of the defect structure of nonstoichiometric cerium dioxide. *Solid State Ionics* 1993;**66**:85–95.
32. Simmons RO, Balluffi RW. Measurements of equilibrium vacancy concentrations in aluminum. *Phys Rev* 1960;**117**:52–61.
33. Bishop SR, Kim J-J, Thompson N, Chen D, Kuru Y, Stefanik TS, Tuller HL. Mechanical, electrical, and optical properties of $(Pr,Ce)O_2$ solid solutions: kinetic studies. *ECS Trans* 2011;**35**:1137–44.